

PROGRESS IN LATTICE QCD

Andreas S. Kronfeld

*Theoretical Physics Department, Fermi National Accelerator Laboratory,
Batavia, Illinois, USA*



ABSTRACT

After reviewing some of the mathematical foundations and numerical difficulties facing lattice QCD, I review the status of several calculations relevant to experimental high-energy physics. The topics considered are moments of structure functions, which may prove relevant to search for new phenomena at the LHC, and several aspects of flavor physics, which are relevant to understanding CP and flavor violation.

1 Introduction

Several areas of research in elementary particle physics (as well as nuclear physics and astrophysics) require information about the long-distance nature of quantum chromodynamics (QCD). Sometimes this information can be gleaned from experiment, but often what one needs, in practice, are *ab initio* calculations of the properties of hadrons. In some cases one aims for a detailed understanding of QCD in its own right. In others, one simply requires a reliable calculation of hadronic properties, so that one can study electroweak interactions or new phenomena at short distances.

Mathematical physicists tell us that the best way to define gauge theories, including QCD, is to start with a space-time lattice. The spacing between sites is usually called a . If the finite grid has $N_3 \times N_4$ sites, then one has a finite box size, $L = N_3 a$, and finite extent in time, $L_4 = N_4 a$. Quarks are described by lattice fermion fields located at the sites, denoted $\psi(x)$; gluons are described by lattice gauge fields located on the *links* from x to $x + a\hat{\mu}$, denoted $U_\mu(x)$. The key advantage to the lattice is that local gauge invariance is simple. The fields transform as

$$\psi(x) \mapsto g(x)\psi(x), \quad \bar{\psi}(x) \mapsto \bar{\psi}(x)g^{-1}(x), \quad (1)$$

$$U_\mu(x) \mapsto g(x)U_\mu(x)g^{-1}(x + a\hat{\mu}), \quad (2)$$

so it is easy to devise gauge invariant actions, *i.e.*, independent of $g(x)$ [1]. If one imagines a smooth underlying gauge potential $A_\mu(x)$ (as is used in continuum QCD), the relation to the lattice gauge field is

$$U_\mu(x) = \text{P exp} \int_0^a ds A_\mu(x + s\hat{\mu}). \quad (3)$$

Continuum QCD is defined from lattice QCD by taking $a \rightarrow 0$ with L and hadron masses fixed. Then one takes the infinite volume limit, $L \rightarrow \infty$. If one is interested in the chiral limit, $m_q \rightarrow 0$, it should be taken last. These limits are nothing radical: the lattice provides an ultraviolet cutoff, and the finite volume an infrared cutoff.

The existence of these limits has not been proven rigorously, but, because of asymptotic freedom, there is not much doubt that this procedure works. (If not, why does QCD work at all?) The lattice formulation makes field theory mathematically similar to statistical mechanics and, consequently, provides new tools. For example, a finite lattice makes it possible to integrate the functional integral by Monte Carlo methods. The expectation value of observable Φ may be written

$$\langle \Phi(\phi) \rangle = \frac{1}{Z} \int \mathcal{D}\phi \Phi(\phi) e^{-S(\phi)} \simeq \frac{1}{Z} \sum_i \Phi(\phi^{(i)}) w(\phi^{(i)}) \quad (4)$$

where Z is chosen so that $\langle 1 \rangle = 1$, and ϕ is an abbreviation for all fields, ψ , $\bar{\psi}$, and U . The right-most expression is a numerical approximation, with the sum running over some set of field configurations. This numerical technique, though only one facet of lattice gauge theory, is what most particle physicists mean by “lattice QCD.” So, this talk is about tools need to make numerical calculations more reliable, and the progress being made in calculations needed to interpret “physics in collision.”

It is not so easy to descend from the mathematical high ground down to realistic, practical numerical calculations. Difficulties arise because QCD is a multi-scale problem. Nature has not only the characteristic scale of QCD, Λ_{QCD} , but also a wide range of quark masses, leading to a hierarchy

$$m_q \ll \Lambda_{\text{QCD}} \ll m_Q. \quad (5)$$

As a dynamical scale, rather than a parameter, there is a range for the QCD scale. Some benchmarks include the scale in the running coupling $\Lambda_{\overline{\text{MS}}} \approx 250$ MeV, typical hadron masses like $m_\rho = 770$ MeV, and the scale of chiral symmetry breaking $m_K^2/m_s = 2500$ MeV. The strange quark, with $m_s \approx 100$ MeV, is light, and the up and down quarks, with $\hat{m} = \frac{1}{2}(m_d + m_u) = m_s/24$ and $m_d > m_u > 0$, are especially light. The bottom quark, with $m_b = 4.25$ GeV, is heavy, and the top quark, with $m_t = 175$ GeV, is especially heavy. One can argue whether the charmed quark, with $2m_c = 2.5$ GeV, is heavy or not.

Cutoffs are needed to put the problem on a computer, and they introduce two more scales. The idealized hierarchy is now

$$L^{-1} \ll m_q \ll \Lambda_{\text{QCD}} \ll m_Q \ll a^{-1}. \quad (6)$$

It is impractical to expect a huge separation of scales in computational physics. To explain why, some simple scaling laws are helpful. The memory required grows like $N_S^3 N_4 = L^3 L_4 / a^4$, and these large exponents come because we live in $3 + 1$ space-time dimensions. The CPU time needed to update gauge fields in the Monte Carlo scales like $a^{-(4+z)}$, where $z = 1$ or 2 , and the 4 again comes from the dimension of space-time. The CPU time needed to compute quark propagators scales like m_q^{-p} where $p = 1-3$. The exponents z and p are non-zero because of properties of our numerical algorithms, and it seems difficult to reduce them.

The first consequence of these scaling laws is that a^{-1} can be larger, but not much larger, than Λ_{QCD} . Similarly, m_q and L^{-1} can be smaller, but not much smaller. A more important consequence is that improved methodology pays off enormously. For example, B physics with $a^{-1} \sim 3\Lambda_{\text{QCD}}$ instead of $3m_b$ saves a

factor $(m_b/\Lambda_{\text{QCD}})^6 > 2^{12}$ in computing. Such improvements are not attained by CPU power, but through new ideas. Moreover, in computational physics the need for creativity means that computing facilities must be flexible, not just big.

So, we see that finite computer resources force us to consider the hierarchy

$$L^{-1} < m_q < \Lambda_{\text{QCD}} \ll m_Q \sim a^{-1}, \quad (7)$$

instead of the idealized one. One should emphasize that we know how to get from the practical hierarchy (7) to physical results. The central idea is to let the computer work on dynamics at the scale Λ_{QCD} , and to use effective field theories to get the rest. The computer runs, by necessity, with finite cutoffs and artificial quark masses. With effective field theories, one can strip off the artifice, and replace it with the real world. In doing so, one introduces theoretical uncertainties, but effective field theories control the error analysis.

A more thorough exposition of this line of thinking can be found in a recent review [2]. Here let us emphasize the role of effective field theories by listing some of the big ideas in lattice of the last several years:

- Static limit and lattice NRQCD to treat heavy quarks
- Understanding lattice perturbation theory (to match at short distances)
- Non-perturbative implementation of the Symanzik effective field theory
- Continuum HQET to control heavy-quark discretization effects
- Novel applications of chiral perturbation theory
- Understanding chiral symmetry in lattice gauge theory

All but the last explicitly bring in effective field theories, and it resonates with the usage of chiral perturbation theory to extrapolate light quark masses.

The exception to the rule of effective field theory is something called the quenched approximation. Quenched QCD is a model, so the associated uncertainty is difficult to estimate. For example, unquenched (usually $n_f = 2$ not 3) calculations of hadron masses, decay constants, etc., suggest changes of 0–20%. Fortunately, the quenched approximation is going away. Within a few years, I imagine that quenched calculations will no longer play an important role in our thinking about non-perturbative QCD.

The rest of this paper looks at some calculations needed to interpret current and future experiments. Moments of structure functions can help obtain better

parton densities and, hence, better predictions of cross sections at the Tevatron and LHC. Lattice calculations of these moments are covered in Sec. 2. In flavor physics, the focus of many experiments, there is a pressing need for the hadronic matrix elements needed in leptonic and semi-leptonic decays, and neutral meson mixing. There are many of these, and Sec. 3 covers only a subset: form factors $\mathcal{F}_{B \rightarrow D^*}(1)$ and $f_+(E)$ to obtain $|V_{cb}|$ and $|V_{ub}|$ from $B \rightarrow D^* l \nu$ and $B \rightarrow \pi l \nu$; and matrix elements for neutral B , B_s , and K oscillations, need to constrain V_{td} . Section 4 concludes with a summary and some thoughts about the future.

2 Moments of Structure Functions

The rate for deeply inelastic lp scattering (DIS) depends on several structure functions, which we shall generically denote $F(x)$. x is the momentum fraction of the struck parton, $0 \leq x \leq 1$. In perturbative QCD, the F s can be related to process-independent parton densities, which are used to predict cross sections for $p\bar{p}$ and pp collisions. The DIS data peter out for $x > x_{\max} \sim 0.7$, so, as sketched in Fig. 1(a), the uncertainty explodes for the highest values of x . High x partons are needed to produce high-mass particles. Modern methods for parton densities directly reflect the lack of information [3]. They need independent (but QCD-based) knowledge of the moments to constrain $F(x)$ for $x > x_{\max}$.

The operator product expansion relates the moments to local operators,

$$\int_0^1 dx x^{n-1} F(x, Q^2) = C_n(Q^2/\mu^2) \langle p | \mathcal{O}_n | p \rangle(\mu), \quad (8)$$

where C_n is a short-distance Wilson coefficient that is calculated in perturbation theory. The matrix element on the right-hand side should be “easy” to calculate: just find a lattice operator $\mathcal{O}_{n\text{lat}}$ with the same quantum numbers as \mathcal{O}_n and calculate the

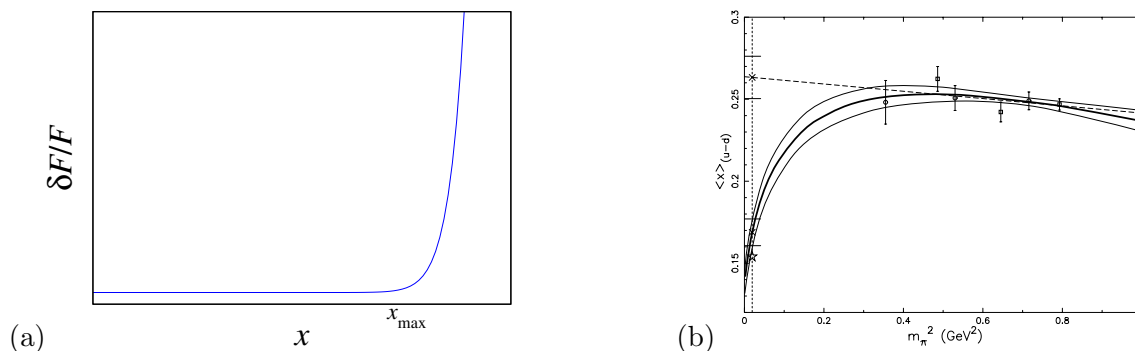


Figure 1: (a) Sketch of the uncertainty in measured structure functions, as a function of x . (b) Comparison of chiral extrapolations for $\langle x \rangle_{u-d}$; from Ref. [10]

matrix element at several different lattice spacings. We have a detailed description of lattice-spacing effects, namely,

$$\begin{aligned} \langle p|O_{n\text{lat}}|p\rangle(a) &= Z_{nm}^{-1}(\mu a)\langle p|\mathcal{O}_m|p\rangle(\mu) + aK_{nj}\langle p|\mathcal{O}'_j|p\rangle \\ &+ aK_{\sigma F}Z_{nm}^{-1}\int d^4x \langle p|T\mathcal{O}_m\bar{q}\sigma Fq(x)|p\rangle + O(a^2), \end{aligned} \quad (9)$$

based on an effective field theory introduced by Symanzik two decades ago [4]. Differences between lattice gauge theory, with $a \neq 0$, and continuum QCD arise at short distances comparable to a . They are lumped into short-distance coefficients Z_{nm} , aK_{nj} , and $aK_{\sigma F}$. The operators on the right-hand side are, in the Symanzik effective field theory, defined with a continuum renormalization. Thus, in addition to calculating the left-hand side, to obtain $\langle p|\mathcal{O}_m|p\rangle$ one must also compute the normalization factor Z_{nm} and cope with the terms of order a .

We know how to calculate Z_{nm} , $K_{\sigma F}$, and K_{nj} . They depend on details of the lattice Lagrangian and the lattice operator $O_{n\text{lat}}$. One can introduce parameters (call them c_{SW} and c_{nj}) that directly influence $K_{\sigma F}$ and K_{nj} . Thus, one can adjust c_{SW} and c_{nj} until $K_{\sigma F} \approx 0$ and $K_{nj} \approx 0$. This procedure is called Symanzik improvement [5]. There are two ways to compute the Z s and K s. One is renormalized perturbation theory, which works because the Z s and K s are short-distance quantities. In this method, uncertainties of order α_s^l remain. Usually, these days, only one-loop calculations are available, so $l = 2$. Then it is helpful to apply the Brodsky-Lepage-Mackenzie prescription [6] to sum up higher-order terms related to renormalization parts. The other method is fully non-perturbative [7]. This sounds as if it is exact, but there are uncertainties in the K s of order a . For the matrix element itself, this is just another error of order a^2 , of which there are many. The first method has been used by the QCDSF collaboration [8], who have rather comprehensive results for the proton. The second method has been used by a Zeuthen-Roma II collaboration [9], for the first moment of the pion structure function.

The quenched results from QCDSF do not agree especially well with phenomenology. It is, of course, tempting (and reasonable) to blame the quenched approximation. Till now, one could also blame the phenomenological result, which gets a significant contribution from the high- x region, where there are no experimental data. As it turns out, neither is the main culprit. Earlier this year the LHPC and Sesam collaborations finished a comparison of quenched and unquenched (well, $n_f = 2$) calculations of many proton moments [10]. To save computer time, these calculations are done with artificially large light quark mass (for the reasons explained above). The dependence on the light quark mass for a typical moment is

shown in Fig. 1(b). Ref. [10] finds hardly any difference between unquenched and quenched calculations for $0.7m_s < m_q < 1.6m_s$. It makes a huge difference, however, whether one follows one's nose and extrapolates linearly, or whether one follows chiral perturbation theory. The latter, of course, is correct. It has a pronounced curvature for small quarks masses, of the form $m_\pi^2 \ln m_\pi^2$ (and $m_\pi^2 \propto m_q$). With chiral perturbation theory, the extrapolated result agrees with phenomenology.

3 Flavor Physics

The central question in flavor physics is whether the standard CKM mechanism explains all flavor and CP violation (in the quark sector). One angle on this question is over-constraint of the CKM matrix. Because the CKM matrix has only four free parameters, the magnitudes of the CKM matrix elements dictate the CP violating phase. Many of the magnitudes may be obtained from semi-leptonic decays, such as $K \rightarrow \pi l \nu$ for the Cabibbo angle, $B \rightarrow D^* l \nu$ for $|V_{cb}|$, and $B \rightarrow \pi l \nu$ for $|V_{ub}|$. CKM elements on the third row (involving the top quark) enter through neutral meson mixing, in the neutral K , B , and B_s systems. Here we will focus on B physics, with a few remarks on K^0 - \bar{K}^0 mixing in Sec. 3.4.

For B physics, one must confront heavy quark discretization effects. Compared to the lattice spacing, the b quark mass is large, $m_b a > 1$. The Symanzik effective field theory, at least as usually applied, breaks down. Lattice gauge theory does not break down, however, and the Isgur-Wise heavy-quark symmetries emerge, in the usual way, for all $m_Q a$ [11]. Thus, as long as $m_Q \gg \Lambda_{\text{QCD}}$, lattice gauge theory can be described by heavy-quark effective theory (HQET). One can write [12]

$$\mathcal{L}_{\text{lat}} \doteq \sum_n \mathcal{C}_n^{\text{lat}}(m_Q, m_Q a; \mu) \mathcal{O}_n(\mu), \quad (10)$$

where \doteq means “has the same matrix elements as.” In the same way

$$\mathcal{L}_{\text{QCD}} \doteq \sum_n \mathcal{C}_n^{\text{cont}}(m_Q; \mu) \mathcal{O}_n(\mu). \quad (11)$$

The difference is in the short-distance coefficients \mathcal{C}_n . On the lattice there are two short distances, a and m_Q^{-1} , so the $\mathcal{C}_n^{\text{lat}}$ depend on the ratio $a/m_Q^{-1} = m_Q a$. On the other hand, the operators \mathcal{O}_n in Eqs. (10) and (11) are essentially the same.

One can therefore systematically improve lattice calculations of b -flavored hadrons, by matching lattice gauge theory and continuum QCD such that

$$\delta \mathcal{C}_n = \mathcal{C}_n^{\text{cont}} - \mathcal{C}_n^{\text{lat}} \approx 0, \quad (12)$$

for the first several operators. HQET is, here, merely an analysis tool; details of how HQET is defined and renormalized drop out of the difference. These ideas are put to direct use in the Fermilab method [11, 12], which is based on Wilson fermions and, thus, also possesses a smooth continuum limit. Similar ideas are put to use in lattice NRQCD [13], which discretizes the continuum heavy-quark Lagrangian.

3.1 $B \rightarrow D^* l \nu$, $\mathcal{F}_{B \rightarrow D^*}(1)$, and $|V_{cb}|$

To determine $|V_{cb}|$ from the semi-leptonic decay $B \rightarrow D^* l \nu$, one measures the differential decay rate in w , which is the velocity transfer from the B to the D^* . Then, one extrapolates to zero recoil, $w = 1$. Thus, one can summarize the experiment by saying it measures $|V_{cb}| \mathcal{F}_{B \rightarrow D^*}(1)$, where $\mathcal{F}_{B \rightarrow D^*}(w)$ is a certain combination of form factors. At zero recoil all form factors but h_{A_1} are suppressed, so

$$\mathcal{F}_{B \rightarrow D^*}(1) = h_{A_1}(1) = \langle D^*(v) | \mathcal{A}^\mu | B(v) \rangle. \quad (13)$$

It should be “straightforward” to calculate this matrix element in lattice QCD. But a brute force calculation of $\langle D^* | \mathcal{A}^\mu | B \rangle$ would not be interesting: similar matrix elements like $\langle 0 | \mathcal{A}^\mu | B \rangle$ and (see below) $\langle \pi | \mathcal{V}^\mu | B \rangle$ have 15–20% errors.

At zero recoil heavy-quark symmetry constrains $h_{A_1}(1)$ to take the form

$$h_{A_1}(1) = \eta_A \left[1 + \delta_{1/m^2} + \delta_{1/m^3} \right], \quad (14)$$

where η_A is a short-distance coefficient, and the δ_{1/m^n} are (principally) long-distance matrix elements in HQET at order $1/m^n$. HQET does not provide the tools to calculate them, but with the insight from matching lattice gauge theory to HQET, we have recently figured out how to do so [14]. Furthermore, since we incorporate heavy-quark symmetry from the outset, and all our uncertainties scale as $h_{A_1} - 1$.

From HQET, the structure of the $1/m_Q^n$ corrections is

$$\delta_{1/m^2} = -\frac{\ell_V}{(2m_c)^2} + \frac{2\ell_A}{(2m_c)(2m_b)} - \frac{\ell_P}{(2m_b)^2} \quad (15)$$

$$\delta_{1/m^3} = -\frac{\ell_V^{(3)}}{(2m_c)^3} + \frac{\ell_A^{(3)}\Sigma + \ell_D^{(3)}\Delta}{(2m_c)(2m_b)} - \frac{\ell_P^{(3)}}{(2m_b)^3} \quad (16)$$

where $\Sigma = 1/(2m_c) + 1/(2m_b)$ and $\Delta = 1/(2m_c) - 1/(2m_b)$. In lattice gauge theory, we seek objects whose heavy-quark expansions contain the ℓ s. From work on the $B \rightarrow D$ form factor [15], we know certain ratios have small enough uncertainties. Moreover, one can show via HQET that [12]

$$\frac{\langle D | \bar{c} \gamma^4 b | B \rangle \langle B | \bar{b} \gamma^4 c | D \rangle}{\langle D | \bar{c} \gamma^4 c | D \rangle \langle B | \bar{b} \gamma^4 b | B \rangle} = \left\{ \eta_V^{\text{lat}} \left[1 - \ell_P \Delta^2 - \ell_P^{(3)} \Delta^2 \Sigma \right] \right\}^2, \quad (17)$$

$$\frac{\langle D^* | \bar{c} \gamma^4 b | B^* \rangle \langle B^* | \bar{b} \gamma^4 c | D^* \rangle}{\langle D^* | \bar{c} \gamma^4 c | D^* \rangle \langle B^* | \bar{b} \gamma^4 b | B^* \rangle} = \left\{ \eta_V^{\text{lat}} \left[1 - \ell_V \Delta^2 - \ell_V^{(3)} \Delta^2 \Sigma \right] \right\}^2, \quad (18)$$

$$\frac{\langle D^* | \bar{c} \gamma^j \gamma_5 b | B \rangle \langle B^* | \bar{b} \gamma^j \gamma_5 c | D \rangle}{\langle D^* | \bar{c} \gamma^j \gamma_5 c | D \rangle \langle B^* | \bar{b} \gamma^j \gamma_5 b | B \rangle} = \left\{ \check{\eta}_A^{\text{lat}} \left[1 - \ell_A \Delta^2 - \ell_A^{(3)} \Delta^2 \Sigma \right] \right\}^2, \quad (19)$$

and one-loop expansions of η_V^{lat} and $\check{\eta}_A^{\text{lat}}$ are available [16]. By calculating the ratios for many combinations of the heavy-quark masses, we can fit to the HQET description on the right hand side to obtain all three ℓ s in δ_{1/m^2} , and three of four $\ell^{(3)}$ s in δ_{1/m^3} . We can then reconstitute $h_{A_1}(1)$ with Eq. (14), finding

$$\mathcal{F}_{B \rightarrow D^*}(1) = h_{A_1}(1) = 0.913_{-0.017}^{+0.024} \pm 0.016_{-0.014-0.016-0.014}^{+0.003+0.000+0.006}, \quad (20)$$

where the uncertainties stem from statistics and fitting, HQET matching, lattice spacing dependence, the chiral extrapolation, and the effect of the quenched approximation. Instead of adding these errors in quadrature, we prefer to take note of a bound, $\mathcal{F}_{B \rightarrow D^*}(1) \leq 1$, and posit a Poisson distribution $P(x) = N x^7 e^{-7x}$, $x = [1 - \mathcal{F}_{B \rightarrow D^*}(1)]/0.087 \geq 0$, for global fits of the CKM matrix [17].

3.2 $B \rightarrow \pi l \nu$, $f_+(E)$, and $|V_{ub}|$

To determine $|V_{ub}|$ from the semi-leptonic decay $B \rightarrow \pi l \nu$, it is not just a rehash of the previous section. The experimental rate is smaller, by a factor $|V_{ub}/V_{cb}|^2$, and heavy-quark symmetry is not as constraining. Experiments should measure [18]

$$\int_{E_l^{\text{min}}}^{E_l^{\text{max}}} dE_l \int_{E_\pi^{\text{min}}}^{E_\pi^{\text{max}}} dE_\pi \frac{d^2 \Gamma}{dE_l dE_\pi} \propto |V_{ub}|^2 \int_{E_\pi^{\text{min}}}^{E_\pi^{\text{max}}} dE_\pi p^3 |f_+(E_\pi)|^2, \quad (21)$$

where $E_\pi = v \cdot p_\pi$ is pion energy in the B rest frame, $p^2 = E_\pi^2 - m_\pi^2$, and E_l is charged lepton energy. To determine $|V_{ub}|$ one needs a reliable calculation of the form factor $f_+(E)$, which parameterizes the matrix element of the $b \rightarrow u$ vector current. Any cut on the lepton variable is equally good [18].

Recently there have been several calculations of these form factors, using several different methods [19, 20, 21, 22, 23]. Two of these works [19, 20] calculate the matrix element with m_Q around the charm mass, fit to a model for the E_π dependence, and extrapolate the model parameters with heavy-quark scaling. The others appeal more directly to heavy-quark ideas, as discussed above. El-Khadra *et al.* [21] use the Fermilab method, and the other two [22, 23] use lattice NRQCD. Refs. [21, 22, 23] do not use a model for the E_π dependence; instead a cut on E_π is used to control discretization effects.

An obvious challenge in these calculations arises from discretization errors of the final-state pion, which grow as $\mathbf{p}_\pi a$. This makes it hard to get $E_\pi = 2.6$ GeV.

A possibility to circumvent this difficulty is to give B meson momentum [24]. For example, if one chooses $-\mathbf{p}_B = \mathbf{p}_\pi = 800$ MeV in the lattice frame of reference, one can access the whole kinematic range. A less obvious, but also important, challenge is the chiral extrapolation. It is not well understood and contributes the largest systematic error in the calculation with the smallest quark masses [21]. The uncertainties on $f_+(E)$ are still 15–20% in the quenched approximation. But there are no real technical roadblocks (for details, see Ref. [21]), so the errors will be reduced while BaBar and Belle accumulate data. In the short term, it will be interesting and important to compare similar lattice calculations for semi-leptonic D decays to experimental results from CLEO- c .

3.3 Neutral B Mixing and $|V_{td}|$

In the Standard Model, neutral meson mixing is sensitive to V_{td} and V_{ts} . A significant recent development is the realization that the theoretical uncertainty in B^0 - \bar{B}^0 mixing has been underestimated. The culprit has been the chiral extrapolation, which we have seen to be important in moments of structure functions.

In the Standard Model, the oscillation frequency for B_d^0 - \bar{B}_d^0 mixing is

$$\Delta m_d \propto |V_{td}|^2 \mathcal{M}_d \quad (22)$$

where $\mathcal{M}_q = \langle \bar{B}_q^0 | [\bar{b}(1 - \gamma_\mu)\gamma_5 q][\bar{b}(1 - \gamma_\mu)\gamma_5 q] | B_q^0 \rangle$. Phenomenologists usually write $\mathcal{M}_q = \frac{8}{3} m_{B_q}^2 f_{B_q}^2 B_{B_q}$ but lattice calculations give matrix elements \mathcal{M}_q directly, and f_{B_q} from $\langle 0 | \bar{b}\gamma_\mu\gamma_5 q | B_q^0 \rangle$. Nevertheless, it turns out to be useful to look separately at f_{B_q} and B_{B_q} . Current world averages (from lattice QCD) are $f_{B_q} = 198 \pm 30$ MeV and $B_{B_q} = 1.30 \pm 0.12$ [25]. So the error on $|V_{td}|$ from Δm_d alone is $\sim 15\%$.

For some time, the conventional wisdom has said that most of the theoretical uncertainty cancels if one takes the ratio $\Delta m_s/\Delta m_d$. (It is anticipated that Δm_s will be measured at Run 2 of the Tevatron [26].) The ratio is

$$\frac{\Delta m_s}{\Delta m_d} = \left| \frac{V_{ts}}{V_{td}} \right|^2 \frac{m_{B_s}}{m_{B_d}} \xi^2, \quad \xi^2 = \frac{f_{B_s}^2 B_{B_s}}{f_{B_d}^2 B_{B_d}}. \quad (23)$$

CKM unitarity says $|V_{ts}| = |V_{cb}|$ to good approximation, and $|V_{cb}|$ is known to 2–4%. Many authors believe the uncertainty in ξ to be less than 5%. Cancellations do occur in the statistical error, and in systematics at short distances (a and m_b^{-1}) and—arguably—at medium distances ($\Lambda_{\text{QCD}}^{-1}$). But they explicitly do *not* cancel at long distances between m_s^{-1} and m_d^{-1} from light quarks in the B_s and B mesons.

Now, the quenched approximation does not work well at these long distances, and unquenched calculations are prohibitive at $m_q \sim m_d$. Thus, ξ isolates

the contributions that are hardest to capture, and tries to get at them by extrapolating in m_q . After studying the differences in chiral logarithms in real QCD and the quenched approximation, Booth [27] and Sharpe and Zhang [28] sounded notes of caution. Their analyses showed that chiral logarithms should induce curvature as a function of light quark mass, which quenching would obscure. This curvature has recently been observed in unquenched calculations (well, $n_f = 2$ again), and identified as a serious source of uncertainty [29].

It is not too difficult to grasp the problem. For convenience, let $\xi = \xi_f \xi_B$, where $\xi_f = f_{B_s}/f_{B_d}$, $\xi_B^2 = B_{B_s}/B_{B_d}$. Chiral perturbation theory says that

$$\xi_f(r) - 1 = m_{ss}^2(1-r) \left[\frac{1}{2}f_2 - \frac{1 + 3g_{BB^*\pi}^2}{(4\pi f_\pi)^2} l(r) \right], \quad (24)$$

where $m_{ss}^2 = 2m_K^2 - m_\pi^2$, $r = m_q/m_s$ measures the light quark mass in units of the strange mass, f_π is the pion decay constant, and $g_{BB^*\pi}$ is the B - B^* - π coupling. The function $l(r)$ contains chiral logarithms:

$$(1-r)l(r) = \frac{1}{4}(1+r) \ln[(1+r)/2] + \frac{1}{12}(2+r) \ln[(2+r)/3] - \frac{3}{4}r \ln(r)$$

B_s mixing:	$B_s \leftrightarrow B^*K$	$B_s \leftrightarrow B_s^*\eta$	
B_d mixing:	$B \leftrightarrow B_s^*K$	$B \leftrightarrow B^*\eta$	$B \leftrightarrow B^*\pi$

(25)

and each term arises from the virtual corrections given beneath it. All other contributions are described well enough by linear behavior in r and are lumped into the constant f_2 . The ratio ξ_B^2 is described by an expression similar to Eq. (24), except that the chiral log is multiplied by $1 - g_{BB^*\pi}^2$. Unquenched lattice calculations [29, 30] are not yet good enough to determine directly the coefficients of the chiral logs. Sinéad Ryan and I have suggested taking them from phenomenology instead [31]. We invoke heavy-quark symmetry, which says the B - B^* - π coupling should be roughly the same as the D - D^* - π coupling. Then the recent measurement of the D^* width yields $g_{DD^*\pi}^2 = 0.35$ [32]; we take $g_{BB^*\pi}^2 = 0.35 \pm 20\%$. We obtain the constant f_2 from the slope of $\xi_f(r)$ around $0.5 < r < 1.0$, where quenched and unquenched calculations are in good agreement. We also analyze ξ_B^2 in the same manner. Finally, we find

$$\xi = 1.32 \pm 0.10 \quad (\text{chiral log extrapolation}) \quad (26)$$

from the chiral log fit. Previously, one had tried linear fits, which would have given

$$\xi = 1.15 \pm 0.05 \quad (\text{conventional linear extrapolation}) \quad (27)$$

for the same input. The difference is illustrated in Fig. 2(a). One sees that the uncertainty of 5% [as in Eq. (27)] certainly was underestimated, and also that the central value is probably quite different from the conventional 1.15.

3.4 Kaon Physics

Two theoretical developments of the past few years have opened the way for a wider range of kaon calculations. One is a method for exploiting finite-volume effects to calculate phase shifts in $K \rightarrow \pi\pi$ (and other quasi-elastic processes) [33]. The other is the formulation of lattice fermions with good chiral symmetry [34, 35, 36]. With these new tools, we may be able to obtain, at last, quantitative results for such long-standing problems as the $\Delta I = \frac{1}{2}$ rule and the matrix elements needed to compute ε'/ε in the Standard Model.

Ref. [33] (and earlier papers by Lüscher) base a formalism for calculating final-state phases on three insights. The first is that energy levels in finite volumes are discrete. The second is that phase shifts arise at hadronic distances of order 1 fm, remote from the box size $L > 1$ fm. Lastly, there is a kinematical, albeit very non-trivial, set of L -dependent relationships between the phase shifts and the energy levels. As a result, one can extract the (elastic) phase shifts from the L dependence of the discrete energy spectrum. Unfortunately, practical application to QCD requires box sizes $L = 2\text{--}6$ fm, so it will not be feasible soon.

In many kaonic matrix elements, chiral symmetry is important, for example for maintaining a simple relation between lattice operators and their counterparts in continuum QCD. In 1982 Ginsparg and Wilson derived a sufficient condition for chiral symmetry on the lattice [37]. For a long time the Ginsparg-Wilson relation defied solution, but now there are at least two realizations, the “fixed-point action” [35], and “overlap fermions” [36]. Another method, “domain-wall fermions” [34], is related to the former and has exponentially small violations of the Ginsparg-Wilson relation. Two lattice collaborations have large-scale calculations of B_K (defined

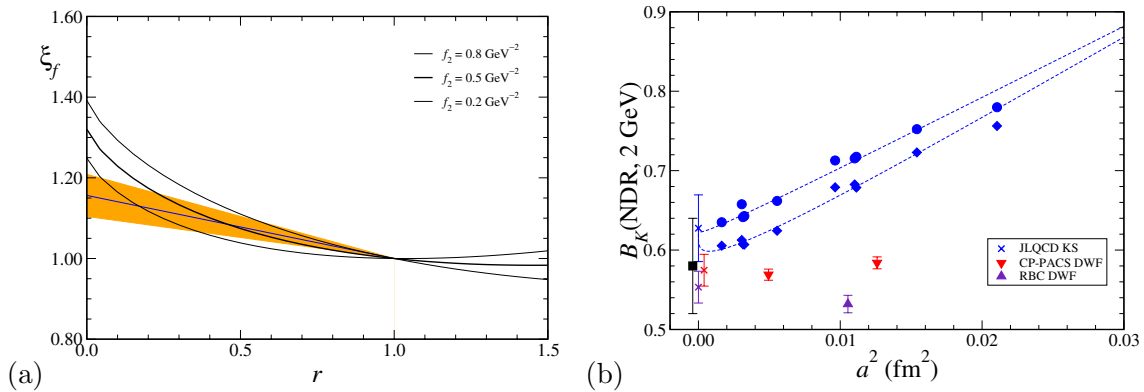


Figure 2: Neutral meson mixing. (a) Comparison of chiral extrapolations of ξ [31]. (b) B_K vs. a^2 , with results from JLQCD [40], CP-PACS [38], and RBC [39].

analogously to B_B) with domain-wall quarks. In Fig. 2, published results from CP-PACS [38] and RBC [39] are compared to classic work of JLQCD (with Kogut-Susskind quarks) [40]. The lattice spacing dependence seems gentler for domain-wall fermions. From looking at the plot, a rough estimate of an average would be

$$B_K(\text{NDR}, 2 \text{ GeV}) = 0.58 \pm 0.06 \quad (28)$$

which encompasses also Ref. [41]. This uncertainty could easily be reduced, by using, say, 3–5 lattice spacings with domain-wall (or overlap) fermions, and taking the continuum limit. One should also keep in mind that these calculations have been done in the quenched approximation, and with degenerate quarks of mass $m_s/2$.

4 Conclusions and Prospects

Although the foundation of lattice QCD is sound, some difficulties arise when turning the idealized theory into a computation tool. Errors are introduced at short and long distances. They are controlled by effective field theories, however, providing reliable methods to obtain physical predictions. A wide variety of calculations in the quenched approximation have allowed us to learn how control short-distance effects: both for light quarks and for heavy quarks. Now that several (partially) unquenched calculations are available, other issues are becoming clearer, particularly the chiral extrapolation of light quark masses. One can be optimistic that unquenched calculations—with solid, transparent analyses of all uncertainties—will become available to help interpret experiments with high-energy collisions.

One upcoming program is especially noteworthy vis a vis lattice QCD. In the next few years, CLEO-*c* [42] will measure leptonic and semi-leptonic decays of D and D_s mesons to a few per cent. Lattice QCD has a chance to predict their results, perhaps with comparable accuracy. An especially interesting combination is $f_+^{D \rightarrow Kl\nu}(E)/f_{D_s}$ (and the Cabibbo-suppressed cousin $f_+^{D \rightarrow \pi l\nu}(E)/f_D$). The CKM matrix drops out from the measurements, and non-Standard physics is unlikely. Thus, one has direct tests of non-perturbative QCD. The ratio f_{D_s}/f_D is also interesting, because it tests the chiral extrapolation of ξ in B - \bar{B} mixing. Successful comparisons of lattice calculations and CLEO-*c* will give confidence in other applications of lattice QCD, such as B physics and moments of the parton densities.

Acknowledgments

Fermilab is operated by Universities Research Association Inc., under contract with the U.S. Department of Energy.

References

1. K. G. Wilson, Phys. Rev. D **10**, 2445 (1974).
2. A. S. Kronfeld, Uses of effective field theory in lattice QCD, in: At the Frontiers of Particle Physics: Handbook of QCD, (ed. M. Shifman) **4**, (World Scientific, Singapore, 2002) [arXiv:hep-lat/0205021].
3. W. T. Giele, S. A. Keller, and D. A. Kosower, arXiv:hep-ph/0104052.
4. K. Symanzik, Cutoff dependence in lattice ϕ^4 in four dimensions theory, in: Recent Developments in Gauge Theories, (ed. by G. 't Hooft *et al.*, Cargese, August 1979) **59**, 313 (Plenum, New York, 1980).
5. K. Symanzik, Some topics in quantum field theory, in: Mathematical Problems in Theoretical Physics, (ed. by R. Schrader *et al.*, Hamburg, August 1981) **6**, 47 (Springer, New York, 1982); Nucl. Phys. B **226**, 187, 205 (1983).
6. S. J. Brodsky, G. P. Lepage, and P. B. Mackenzie, Phys. Rev. D **28**, 228 (1983); G. P. Lepage and P. B. Mackenzie, Phys. Rev. D **48**, 2250 (1993) [arXiv:hep-lat/9209022].
7. For references and a review, see S. Sint, Nucl. Phys. B Proc. Suppl. **94**, 79 (2001) [arXiv:hep-lat/0011081], or Ref. [2].
8. M. Göckeler *et al.*, Phys. Rev. D **53**, 2317 (1996) [arXiv:hep-lat/9508004]; Phys. Lett. B **414**, 340 (1997) [arXiv:hep-ph/9708270].
9. M. Guagnelli, K. Jansen, and R. Petronzio, Phys. Lett. B **493**, 77 (2000) [arXiv:hep-lat/0009006].
10. D. Dolgov *et al.* [LHPC and SESAM Collaborations], Phys. Rev. D **66**, 034506 (2002) [arXiv:hep-lat/0201021].
11. A. X. El-Khadra, A. S. Kronfeld, and P. B. Mackenzie, Phys. Rev. D **55**, 3933 (1997) [arXiv:hep-lat/9604004].
12. A. S. Kronfeld, Phys. Rev. D **62**, 014505 (2000) [arXiv:hep-lat/0002008].
13. G. P. Lepage and B. A. Thacker, Nucl. Phys. B Proc. Suppl. **4**, 199 (1987); B. A. Thacker and G. P. Lepage, Phys. Rev. D **43**, 196 (1991); G. P. Lepage, L. Magnea, C. Nakhleh, U. Magnea, and K. Hornbostel, *ibid.* **46**, 4052 (1992) [arXiv:hep-lat/9205007].

14. S. Hashimoto, A. S. Kronfeld, P. B. Mackenzie, S. M. Ryan, and J. N. Simone, Phys. Rev. D **66**, 014503 (2002) [arXiv:hep-ph/0110253].
15. S. Hashimoto, A. X. El-Khadra, A. S. Kronfeld, P. B. Mackenzie, S. M. Ryan, and J. N. Simone, Phys. Rev. D **61**, 014502 (2000) [arXiv:hep-ph/9906376].
16. J. Harada, S. Hashimoto, A. S. Kronfeld, and T. Onogi, Phys. Rev. D **65**, 094514 (2002) [arXiv:hep-lat/0112045].
17. A. S. Kronfeld, P. B. Mackenzie, J. N. Simone, S. Hashimoto, and S. M. Ryan, in *Flavor Physics and CP Violation*, edited by R. G. C. Oldemann, arXiv:hep-ph/0207122.
18. I thank Andreas Warburton for discussions on this point.
19. K. C. Bowler *et al.* [UKQCD Collaboration], Phys. Lett. B **486**, 111 (2000) [arXiv:hep-lat/9911011].
20. A. Abada *et al.*, Nucl. Phys. B **619**, 565 (2001) [arXiv:hep-lat/0011065].
21. A. X. El-Khadra, A. S. Kronfeld, P. B. Mackenzie, S. M. Ryan, and J. N. Simone, Phys. Rev. D **64**, 014502 (2001) [arXiv:hep-ph/0101023].
22. S. Aoki *et al.* [JLQCD Collaboration], Phys. Rev. D **64**, 114505 (2001) [arXiv:hep-lat/0106024].
23. J. Shigemitsu, S. Collins, C. T. H. Davies, J. Hein, R. R. Horgan, and G. P. Lepage, arXiv:hep-lat/0207011.
24. K. Foley, poster at the XXth International Symposium on Lattice Field Theory, (June 2002, Cambridge, Mass.).
25. S. Ryan, Nucl. Phys. B Proc. Suppl. **106** (2002) 86 [arXiv:hep-lat/0111010].
26. K. Anikeev *et al.*, *B* physics at the Tevatron: Run II and beyond, arXiv:hep-ph/0201071 [FERMILAB-PUB-01-197].
27. M. J. Booth, Phys. Rev. D **51** (1995) 2338 [arXiv:hep-ph/9411433].
28. S. R. Sharpe and Y. Zhang, Phys. Rev. D **53** (1996) 5125 [arXiv:hep-lat/9510037].

29. N. Yamada *et al.* [JLQCD Collaboration], Nucl. Phys. B Proc. Suppl. **106** (2002) 397 [arXiv:hep-lat/0110087]; talk at the CERN workshop on the CKM Unitarity Triangle, (February 2002, Geneva), <http://ckm-workshop.web.cern.ch/>.
30. C. Bernard *et al.* [MILC Collaboration], arXiv:hep-lat/0206016.
31. A. S. Kronfeld and S. M. Ryan, Phys. Lett. B **543**, 59 (2002) [arXiv:hep-ph/0206058]; arXiv:hep-lat/0209083.
32. A. Anastassov *et al.* [CLEO Collaboration], Phys. Rev. D **65** (2002) 032003 [arXiv:hep-ex/0108043].
33. L. Lellouch and M. Lüscher, Commun. Math. Phys. **219**, 31 (2001) [arXiv:hep-lat/0003023].
34. D. B. Kaplan, Phys. Lett. B **288**, 342 (1992) [arXiv:hep-lat/9206013]; Y. Shamir, Nucl. Phys. B **406**, 90 (1993) [arXiv:hep-lat/9303005].
35. U. J. Wiese, Phys. Lett. B **315**, 417 (1993) [arXiv:hep-lat/9306003]; P. Hasenfratz, V. Laliena, and F. Niedermayer, *ibid.* **427**, 125 (1998) [arXiv:hep-lat/9801021].
36. H. Neuberger, Phys. Lett. B **417**, 141 (1998) [arXiv:hep-lat/9707022]; **427**, 353 (1998) [arXiv:hep-lat/9801031].
37. P. H. Ginsparg and K. G. Wilson, Phys. Rev. D **25**, 2649 (1982).
38. A. Ali Khan *et al.* [CP-PACS Collaboration], Phys. Rev. D **64**, 114506 (2001) [arXiv:hep-lat/0105020].
39. T. Blum *et al.* [RBC Collaboration], arXiv:hep-lat/0110075.
40. S. Aoki *et al.* [JLQCD Collaboration], Phys. Rev. Lett. **80** (1998) 5271 [arXiv:hep-lat/9710073].
41. G. Kilcup, R. Gupta, and S. R. Sharpe, Phys. Rev. D **57** (1998) 1654 [arXiv:hep-lat/9707006].
42. R. A. Briere *et al.*, CLEO-*c* and CESR-*c*: A New Frontier of Weak and Strong Interactions, CLNS-01-1742.